MOLECULAR FRONTIERS JOURNAL

Green Synthesis and Scale-Up of MOFs for Water Harvesting from Air

Zhiling Zheng[1,2,3,*], Ali H. Alawadhi[1,2,3] and Omar M. Yaghi[1,2,3]

The synthetic scalability of water harvesting metal–organic frameworks (MOFs) is crucial for making these promising materials accessible and widely available for use in household devices. Herein, we present a facile, sustainable, and high-yield synthesis method to produce a series of water-harvesting MOFs, including MOF-303, CAU-23, MIL-160, MOF-313, CAU-10, and Al-fumarate. Using readily available reactants and water as the only solvent, we were able to synthesize these materials at the kilogram scale in a 200 L batch reactor with yields of 84–96% and space-time yields of 238–305 kg/day/m^3 under optimized reaction conditions. We also show that our procedure preserves framework crystallinity, porosity, and water-harvesting performance of the MOFs synthesized at scale.

Keywords: Metal–Organic Frameworks; Materials; Water Sorption; Green Synthesis; Atmospheric Water Harvesting.

INTRODUCTION

Water scarcity is a major global challenge, with over half the world's population experiencing shortages of this vital resource[1,2]. The temporal and spatial variation in the distribution of available water resources on this planet and the lack of transportation and supplement infrastructure make fresh water even more precious in some arid regions[3,4]. Fortunately, the use of sorbent-assisted atmospheric water harvesting devices has been proposed as a promising solution to address this issue. These devices use porous solid sorbents to trap water molecules at low relative humidity (RH) and release them with minimal energy expenditure[5–8]. Since this approach is neither spatially nor temporally restricted, the supplement of fresh water by the water harvesting device equipped with desirable sorbents can be achieved at any location and at any time of the year[7,9]. However, the development of suitable porous materials for use in these devices, particularly for household use and widespread accessibility, has been a challenge. In addition to having excellent water sorption properties, a desirable sorbent should be scalable, cost-effective, and reproducible in manufacturing in order to be practical for use in various complex real-world conditions[9–11].

Microporous metal–organic frameworks (MOFs) have recently gained attention due to their high tunability, unprecedented variety, and intrinsic porosity, and have been successfully employed in desert water harvesting[5,6,10,12–15]. While a significant body of work has been created in developing MOF sorbents with tailored capacity and isotherm shape, it has largely been limited to small-scale proof of concepts and there are few reports on the large-scale synthesis of water harvesting MOFs for industrial use[16–18]. On the other hand, it was proposed that the concept of green synthesis methods using water as a solvent can address the challenges of high production cost and environmental hazards in the industrial-scale synthesis of MOFs[19–21]. As such, our group has previously

[1]Department of Chemistry, University of California, Berkeley, California, USA. [2]Kavli Energy Nanoscience Institute, University of California, Berkeley, California, USA. [3]Bakar Institute of Digital Materials for the Planet, Division of Computing, Data Science, and Society, University of California, Berkeley, California, USA. *Corresponding author: Zhiling Zheng, Department of Chemistry, University of California, Berkeley, California, USA. E-mail: zn@berkeley.edu. Published online 7 March 2023; doi:10.1142/S2529732523400011

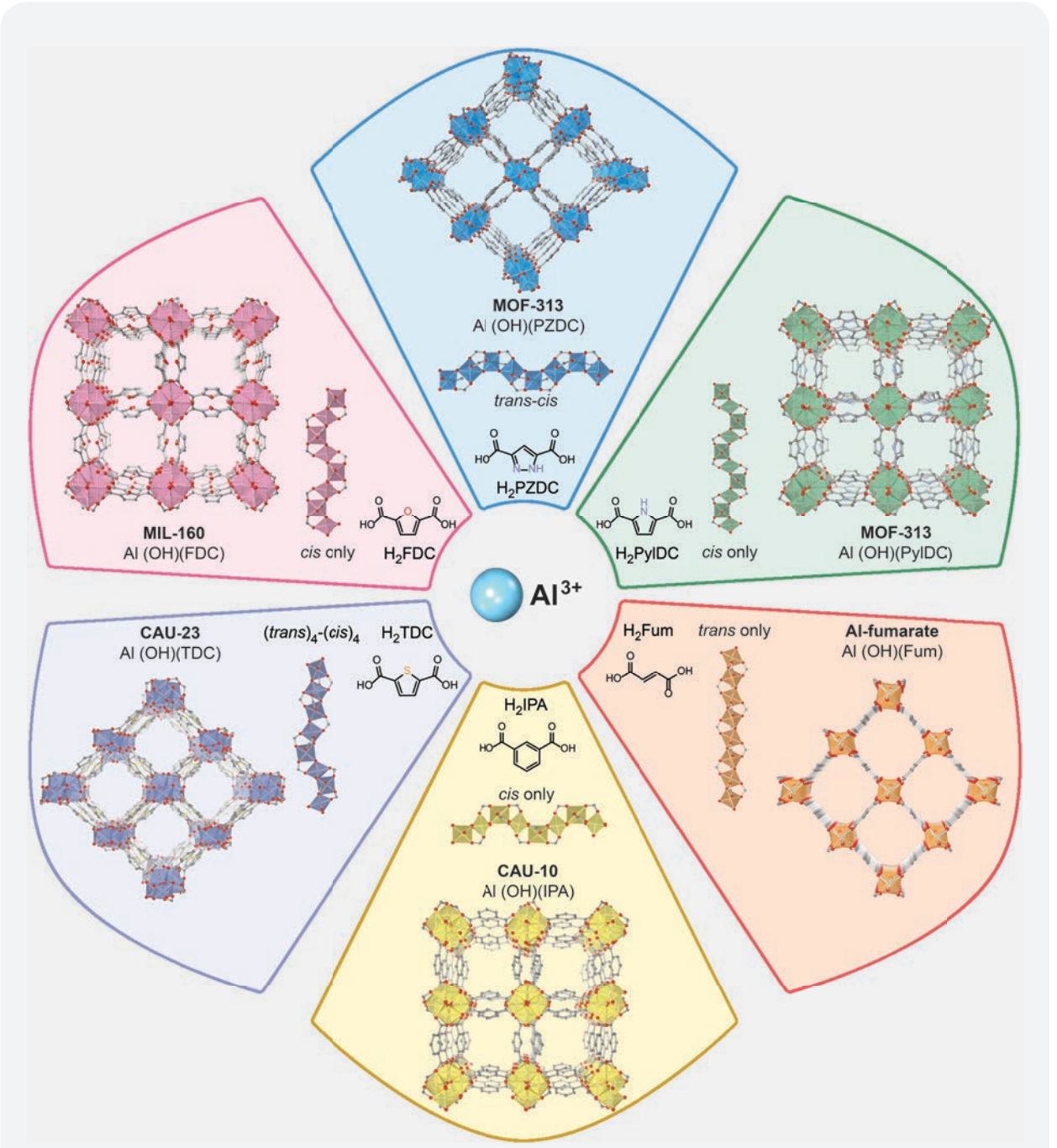

Scheme 1. Illustration of the X-ray diffraction single-crystal structures of relevant MOFs in this work. The aluminum-based MOFs are constructed using ditopic carboxylate linkers with opening angles ranging from 118° to 180°. The rod-like secondary building units (SBUs) consist of cis-only, trans-only, cis–trans-alternating, or $(cis)_4$–$(trans)_4$-alternating corned-shared AlO_6 octahedra (variously colored in different MOFs). Graphics are produced from .cif files Al^{3+} reported in the literature[24,26,31–33]; Color code: O, red; C, gray; N, purple; S, orange. H atoms are omitted for clarity.

developed a green, scalable, and cost-effective method for the synthesis of aluminum-based MOFs on a kilogram scale using inexpensive and readily available starting materials[22,23].

In this report, we further demonstrate that our large-scale, green, and facile production route is generalizable to the synthesis of a series of important water harvesting MOFs (Scheme 1), including MOF-303 [Al(OH)(PZDC), $PZDC^{2-}$ = 1-*H*-pyrazole-3,5-dicarboxylate][13], CAU-23 [Al(OH)(TDC), TDC^{2-} = thiophene-2,5-dicarboxylate][24],MIL-160[Al(OH)(FDC),FDC^{2-}= furan-2,5,-dicarboxylate][25], MOF-313 [Al(OH)(2,5-PylDC),

2,5-PyIDC^{2-} = pyrrole-2,5-dicarboxylate][26,27], Al-fumarate [Al(OH)(Fum), Fum^{2-} = furmarate][28,29], and CAU-10 [Al(OH)(*IPA*), IPA^{2-} = 1,4-benzenedicarboxylate][30]. With this facile water-based synthesis method, each MOF can be produced up to several kilograms per batch, and the materials retain their crystallinity, porosity, and water uptake upon scaling up.

EXPERIMENTAL METHODS AND MATERIALS

Starting materials and general procedures

Bulk (40 kg) 1*H*-pyrazole-3,5-dicarboxylic acid ($H_2PZDC{\cdot}H_2O$, purity ≥ 95%), $AlCl_3{\cdot}6H_2O$ (purity ≥ 99%), and $Al_2(SO_4)_3{\cdot}18H_2O$ (purity ≥ 98%) were purchased from Aaron Chemicals LLC. Bulk (10 kg) 2,5-thiophenedicarboxylic acid (H_2TDC, purity ≥ 98%) was purchased from Ambeed, Inc. Bulk (5 kg) 2,5-furandicarboxylic acid (H_2FDC, purity ≥ 98%), isophthalic acid (purity ≥ 98%), and fumaric acid (purity ≥ 98%) were purchased from Arctom Chemicals LLC. Bulk (20 kg) sodium hydroxide pellets (NaOH, purity ≥ 97%) was purchased from Oakwood Products, Inc. Bulk ethanol (EtOH, purity ≥ 99.8%) was purchased from Sigma Aldrich. 1*H*-Pyrrole-2,5-dicarboxylic acid (H_2PyIDC, purity ≥ 98%) was purchased from Aaron Chemicals LLC. Deuterated solvents were obtained from Cambridge Isotope Laboratories. Ultrahigh-purity (UHP) grade (99.999%) argon and nitrogen were obtained from Praxair. All starting materials and solvents were used without further purification.

Prior to the analysis and characterization, the MOF samples were washed with H_2O and ethanol, and evacuated at room temperature for 1 hour and at 120°C for an additional 12 hour. To analyze the linker composition of the MOF compounds with nuclear magnetic resonance (NMR) spectroscopy, the activated sample was fully hydrolyzed using a NaOD solution (10% in D_2O). ^{1}H-NMR spectra were acquired on Bruker NEO-500 MHz spectrometers, and elemental analysis (EA) was performed on a PerkinElmer 2400 Series II CHNS elemental analyzer at the NMR facility and Microanalytical Laboratory of the College of Chemistry, University of California, Berkeley. Thermal gravimetric analysis (TGA) curves were taken using a TA Q500 thermal analysis system with a heating rate of 5°C/min under N_2 flow. Powder X-ray diffraction (PXRD) patterns were recorded using a Rigaku MiniFlex 6G equipped with a HyPix-400MF Hybrid Pixel Array detector and a normal focus X-ray tube with a Cu-source (λ = 1.54178 Å). Nitrogen sorption experiments were conducted using a Micromeritics Accelerated Surface Area and Porosimetry (ASAP) 2420 System. During the measurement, the sample was cooled to 77 K in a liquid nitrogen bath. Water vapor sorption experiments were carried out on a BEL Japan BELSORP-aqua or a Micromeritics 3Flex Surface Characterization Analyzer. The water vapor source was degassed through five freeze-pump-thaw cycles before the analysis. An isothermal water bath was employed to keep the sample temperature during the measurements.

General preparation of MOF materials

MOF-303, Al(OH)(PZDC). The synthesis of MOF-303 was adopted from our previous reports[22,34]. In a 200 L glass reaction vessel equipped with a heating jacket, a mixture of $H_2PZDC{\cdot}H_2O$ (3.48 kg, 20 mol) and NaOH (2.4 kg, 60 mol) was dissolved in 38 L deionized water. The resulting solution was stirred for 60 minutes until all the solids were completely dissolved and the solution cooled down to room temperature. Next, in a 20 L beaker, $AlCl_3{\cdot}6H_2O$ (4.82 kg, 20 mol) was dissolved in 12 L deionized water and transferred to a 15 L glass material-feeding funnel. The 12 L aluminum chloride solution was slowly added to the 38 L linker solution in the vessel at a rate of 6 L per hour with vigorous stirring. The total addition time lasted 2 hours, and the white precipitate formed during the addition. Afterward, the temperature of the heating jacket was set to 120°C, thus heating the reaction mixture to 100°C. After refluxing for 6 hours and letting the reaction mixture cool down to 60°C, the white solid product was collected in a 20 L filtration funnel. For purification, the white powder was subsequently redispersed by stirring in 15 L aqueous 70% EtOH (v/v) solution, filtered off, and washed again with 30 L anhydrous EtOH at room temperature, followed by filtration and drying under air overnight. The obtained white powder was placed in a 120°C oven for 48 hours to yield the pure and desolvated product (3.61 kg, 91% based on the linker). EA for the activated sample of MOF-303: Calcd. for $AlC_5H_3N_2O_5$ = Al(OH)(PZDC): C, 30.32; H, 1.53; N, 14.14 wt%; Found: C, 29.77; H, 1.58; N, 13.40 wt%.

CAU-23, Al(OH)(TDC). In a 200 L glass reaction vessel equipped with a heating jacket, a mixture of H_2TDC (3.44 kg, 20 mol) and NaOH (2.4 kg, 60 mol) was dissolved in 38 L deionized water. The resulting solution was stirred for 60 minutes until all the solids were completely dissolved and the solution cooled down to room temperature. Next, in a 20 L beaker, $AlCl_3{\cdot}6H_2O$ (4.82 kg, 20 mol) was dissolved in 12 L deionized water and transferred to a 15 L glass material-feeding funnel. The 12 L aluminum chloride solution was slowly added to the 38 L linker solution in the vessel at a rate of 6 L per hour with vigorous stirring. The total addition time lasted 2 hours, and the white precipitate formed during the addition. Afterward, the temperature of the heating jacket was set to 120°C, thus heating the reaction mixture to 100°C. After refluxing for 6 hours and letting the reaction mixture cool down to 60°C, the white solid product was collected in a 20 L filtration funnel. For purification, the white powder was subsequently redispersed by stirring in 15 L aqueous 70% EtOH (v/v) solution, filtered off, and washed again with 30 L anhydrous EtOH at room temperature, followed by filtration and drying under air overnight. The obtained white powder

was placed in a 120°C oven for 48 hours to yield the pure and desolvated product (3.50 kg, 84% based on the linker). EA for the activated sample of CAU-23: Calcd. for $AlC_6H_3SO_5$ = Al(OH)(TDC): C, 33.66; H, 1.41; N, 37.36; S, 14.97 wt%; Found: C, 33.62; H, 1.48; S, 14.95 wt%.

MIL-160, Al(OH)(FDC). In a 200 L glass reaction vessel equipped with a heating jacket, a mixture of H_2FDC (3.12 kg, 20 mol) and NaOH (2.4 kg, 60 mol) was dissolved in 40 L deionized water. The resulting solution was stirred for 60 minutes until all the solids were completely dissolved and

Table 1. Comparison of synthesis scale of water-harvesting MOFs.

MOF	Composition[a]	Solvent and volume[b]	Conditions	Dry MOF obtained per batch (g)	Yield[d] (%)	Space-time-yield (kg·day^{-1}·m^{-3})	References
Al-fumarate	Al(OH)(Fum)	H_2O (50 L)	Reflux, 6 h	2,970	94	238	this work
		H_2O (0.01 L)	60°C, 2 h	0.4	74	436	35
CAU-10	Al(OH)(IPA)	H_2O (50 L)	Reflux, 6 h	3,810	92	305	this work
		H_2O (8.19 L), EtOH (0.42 L)	Reflux, 10 h	500[c]	93	139	16
CAU-23	Al(OH)(TDC)	H_2O (50 L)	Reflux, 6 h	3,610	84	289	this work
		H_2O (0.13 L)	Reflux, 6 h	5	84	154	36
Co-CUK-1	$Co_3(OH)_2(2,4\text{-}PDC)_2$	H_2O (0.004 L)	200°C, 15 h	0.2	67	80	37
MIL-101-Cr	$Cr_3O(OH)(BDC)_3$	H_2O (2.4 L)	200°C, 15 h	127	68	85	38
MIL-125-NH_2	$Ti_8O_8(OH)_4(BDC\text{-}NH_2)_6$	DMF (0.05 L), MeOH (0.01 L)	110°C, 5 h	4	94	320	39
MIL-160	Al(OH)(FDC)	H_2O (50 L)	Reflux, 6 h	3,640	92	291	this work
		H_2O (1 L)	Reflux, 24 h	130[c]	93	130	40
MIP-200	$Zr_6O_4(OH)_4(MDIP)_2(HCOO)_4$	Ac_2O (0.035 L), HCOOH (0.025 L)	120°C, 48 h	1	96	7	41
MOF-303	Al(OH)(PZDC)	H_2O (50 L)	Reflux, 6 h	3,590	91	287	this work
		H_2O (0.75 L)	100°C, 24 h	3	35	4	13
MOF-313	Al(OH)(2,5-PyIDC)	H_2O (0.5 L)	Reflux, 6 h	38	96	304	this work
		H_2O (0.05 L)	Reflux, 12 h	2	93	80	26
		H_2O (0.005 L)	100°C, 2 h	0.01	7	24	27
MOF-801	$Zr_6O_4(OH)_4(HCOO)_6$	DMF (0.04 L), HCOOH (0.01 L)	130°C, 10 h	2	25	96	13
MOF-841	$Zr_6O_4(OH)_4(MTB)_2(HCOO)_4$	DMF (0.04 L), HCOOH (0.02 L)	130°C, 48 h	0.1	55	0.8	5
Ni-BTDD	$Ni_2Cl_2(BTDD)$	DMF (0.2 L), EtOH (0.2 L)	65°C, 10 d	0.3	87	0.1	42
UiO-66	$Zr_6O_4(OH)_4(BDC)_6$	DMF (60 L)	115°C, 24 h	1560[c]	93	26	17

[a]Formula excluding guests. Abbreviations: Fum: fumarate, IPA: 1,3-benzenedicarboxylate (isophthalate), TDC: thiophene-2,5-dicarboxylate, 2,4-PDC: pyridine-2,4-dicarboxylate, BDC: benzene-1,4-dicarboxylate, BDC-NH_2: 2-amine-1,4-benzenedi-carboxylate, FDC: furan-2,5,-dicarboxylate, MDIP: methylene-diisophthalate, $HCOO^-$: formate, PZDC: 1*H*-pyrazole-3,5-dicarboxylate, 2,5-PyIDC: pyrrole-2,5-dicarboxylate, MTB: 4,4′,4″,4‴-methane-tetrayltetrabenzoate, BTDD: bis(1*H*-1,2,3-triazolo[4,5-b],[4′,5′-i])dibenzo[1,4]dioxin, BDC: 1,4-benzenedicarboxylate.

[b]The volume of the modulators, which is much lower than that of other solvents in the reaction, was not listed. EtOH = ethanol, MeOH = methanol, DMF = N,*N*-Dimethylformamide, and HCOOH = formic acid.

[c]The exact weight of dry MOF obtained per batch was not given, and the number was calculated based on the reaction yield.

[d]Yield of each MOF based on the amounts of corresponding linkers.

the solution cooled down to room temperature. Next, in a 20 L beaker, $AlCl_3{\cdot}6H_2O$ (4.82 kg, 20 mol) was dissolved in 10 L deionized water and transferred to a 15 L glass material-feeding funnel. The 10 L aluminum chloride solution was slowly added to 40 L linker solution in the vessel at a rate of 5 L per hour with vigorous stirring. The total addition time lasted 2 hours, and the white precipitate formed during the addition. Afterward, the temperature of the heating jacket was set to 120°C, thus heating the reaction mixture to 100°C. After refluxing for 6 hours and letting the reaction mixture cool down to 60°C, the white solid product was collected in a 20 L filtration funnel. For purification, the white powder was subsequently redispersed by stirring in 15 L aqueous 70% EtOH (v/v) solution, filtered off, and washed again with 30 L anhydrous EtOH at room temperature, followed by filtration and drying under air overnight. The obtained white powder was placed in a 120°C oven for 48 hours to yield the pure and desolvated product (3.64 kg, 92% based on the linker). EA for the activated sample of MIL-160: Calcd. for $AlC_6H_3O_6$ = Al(OH)(FDC): C, 36.38; H, 1.53 wt%; Found: C, 36.49; H, 1.48 wt%.

MOF-313, Al(OH)(2,5-PyIDC). In a 1 L glass round bottom flask, a mixture of H_2PyIDC (31 g, 0.2 mol) and NaOH (24 g, 0.6 mol) was dissolved in 0.4 L deionized water. The resulting solution was stirred for 10 minutes until all the solids were completely dissolved. Next, $AlCl_3{\cdot}6H_2O$ (48.2 g, 0.2 mol) was dissolved in 0.1 L deionized water and added to the round bottom flask dropwise with vigorous stirring. The total addition time lasted 2 hours, and the white precipitate formed during the addition. Afterward, the reaction mixture was heated to 120°C. After refluxing for 6 hours and letting the reaction mixture cool down to room temperature, the white solid product was collected by centrifugation. For purification, the white powder was washed twice with deionized water and subsequently washed three times with EtOH. The white solid was air-dried overnight. Full activation of the MOF was conducted *in vacuo* at 120°C for 24 hours, yielding pure and desolvated product (38 g, 96% based on the linker). EA for the activated sample of MOF-313: Calcd. for $AlC_6H_4O_5N$ = Al(OH)(2,5-PyIDC): C, 36.57; H, 2.05; N, 7.11 wt%; Found: C, 36.55; H, 2.04; N, 6.26 wt%.

Al-fumarate, Al(OH)(Fum). In a 200 L glass reaction vessel equipped with a heating jacket, a mixture of fumaric acid (2.32 kg, 20 mol) and NaOH (2.4 kg, 60 mol) was dissolved in 26 L deionized water. The resulting solution was stirred for 60 minutes until all the solids were completely dissolved and the solution cooled down to room temperature. Next, $AlCl_3{\cdot}6H_2O$ (4.82 kg, 20 mol) was dissolved in 24 L deionized water and divided into two equal portions. The first portion (12 L) was transferred to a 15 L glass material-feeding funnel and subsequently added to the 26 L linker solution in the vessel slowly at a rate of 12 L per hour with vigorous stirring. The procedure was then repeated for the second portion of the aluminum chloride solution. The total addition time lasted for 2 hours, and the white precipitate formed during the addition. Afterward, the temperature of the heating jacket was set to 110°C, thus heating the reaction mixture to 100°C. After refluxing for 6 hours and letting the reaction mixture cool down to room temperature, the white solid product was collected in a 20 L filtration funnel. For purification, the white powder was subsequently redispersed by stirring in 15 L aqueous 70% EtOH (v/v) solution, filtered off, and washed again with 30 L anhydrous EtOH at room temperature, followed by filtration and drying in air overnight. The obtained white powder was placed in a 120°C oven for 48 hours to yield the pure and desolvated product (2.97 kg, 94% based on the linker). EA for the activated sample of Al-fumarate: Calcd. for $AlC_4H_3O_5$ = Al(OH)(Fum): C, 30.40; H, 1.91 wt%; Found: C, 30.28; H, 1.95 wt%.

CAU-10, Al(OH)(IPA). In a 200 L glass reaction vessel equipped with a heating jacket, a mixture of isophthalic acid (3.32 kg, 20 mol) and NaOH (2.4 kg, 60 mol) was dissolved in 26 L deionized water. The resulting solution was stirred for 60 minutes until all the solids were completely dissolved and the solution cooled down to room temperature. Next, $Al_2(SO_4)_3{\cdot}18H_2O$ (6.67 kg, 10 mol) was dissolved in 24 L deionized water and divided into two equal portions. The first portion (12 L) was transferred to a 15 L glass material-feeding funnel and subsequently added to the 26 L linker solution in the vessel slowly at a rate of 12 L per hour with vigorous stirring. The procedure was then repeated for the second portion of the aluminum sulfate solution. The total addition time lasted 2 hours, and the white precipitate formed during the addition. Afterward, the temperature of the heating jacket was set to 130°C, thus heating the reaction mixture to 100°C. After refluxing for 6 hours and letting the reaction mixture cool down to room temperature, the white solid product was collected in a 20 L filtration funnel. For purification, the white powder was subsequently redispersed by stirring in 15 L deionized water, filtered off, and washed again with 3 × 15 L anhydrous EtOH at room temperature, followed by filtration and drying in air overnight. The obtained white powder was placed in a 120°C oven for 48 hours to yield the pure and desolvated product (3.81 kg, 92% based on the linker). EA for the activated sample of CAU-10: Calcd. for $AlC_4H_3O_5$ = Al(OH)(IPA): C, 46.17; H, 2.42 wt%; Found: C, 45.85; H, 2.35 wt%.

RESULTS AND DISCUSSION

The synthesis scale, condition, and yield of a series of water-harvesting MOFs are summarized in Table 1. In up-scale MOF synthesis, important considerations include linker and metal availability, purity of chemicals, raw material costs, the toxicity of reagents, reaction time, reaction yield, and safety[20,43]. As shown in "Experimental Methods and Materials" section, all six MOFs were prepared from commercially available and relatively cheap linkers and aluminum salts. While linkers

purchased in bulk usually have a lower purity (90~95%), it should be noted that if impurities do not react with Al^{3+} in aqueous solution, it will not affect the quality of the MOF product. On the other hand, minimizing the amount of organic solvent used N,*N*-Dimethylformamide (DMF) is essential when transferring syntheses from the small laboratory to the technical scale, as they are toxic and harmful to the environment and account for a large proportion of the manufacturing cost[16,20,44]. Consequently, we chose water as the solvent and used enough base to fully deprotonate the linker to increase its solubility.

To overcome the low yield and long incubation time associated with traditional solvothermal synthesis of MOFs, we developed a reflux-based synthesis method with vigorous stirring to allow sufficient reaction equilibrium in a faster manner (6 hours). This method also allows for higher concentrations compared to unperturbed solvothermal synthesis, resulting in a twofold increase in space-time-yield[34]. More importantly, while the solvothermal synthesis is not scalable, the reflux method is highly scalable and can be adapted for use in an industrial setting. As such, we first optimized the synthesis conditions in a small laboratory setting (100 mL round bottom flask with oil bath)[22], and then adapt the procedure to a scale-up setting (200 L reaction vessel with heated jacket) for further optimizations (Figure 1a).

During the optimization of the reaction parameters for the synthesis of six aluminum-based MOFs with rod SBUs [Al(L)(OH), where L is the deprotonated linker such as $PZDC^{2-}$, TDC^{2-}, and FDC^{2-}], we found that using exactly three equivalents of NaOH was key to maximizing the yield. Two equivalents of NaOH were used for the full deprotonation of the dicarboxylic acid linker, and one equivalent was used for the formation of the SBU. It is worth noting that, although the formation of high crystalline product can be achieved in a shortperiod of time (1 h), we kept the mixture under reflux for 6 hours in kilogram-scale synthesis with a large solvent volume to achieve full porosity and water uptake and minimize undesirable hysteresis in the water isotherm. Using these optimized conditions, we were able to produce approximately 3 kg of activated MOF per batch with a high yield and good water uptake (Figure 1b), which are comparable to results from gram-scale synthesis reported in the literature[6,10,16,26,35].

The crystallinity of the scaled-up MOF products was investigated by PXRD measurements (Figure 2a). The measured values were in good agreement with the simulation data for each MOF. It should be noted that all materials, after washing, showed high crystallinity, with significant peaks that could be well indexed (Figure S1–S6, Supporting Information). This suggests that the scale-up method, with a suitable refluxing time, does not result in a loss of crystallinity for the MOF materials.

The composition of the six MOFs was analyzed using NMR spectroscopy and elemental analysis. After activation, five of them show only one singlet peak from the corresponding dicarboxylate linker in the range of 6.3–7.2 ppm in their ^{1}H digestion NMR (Figure S7–S10 and Figure S12, Supporting Information). CAU-10 showed three peaks from its IPA linker in the range of 7.4–8.1 ppm in its ^{1}H digestion NMR (Figure S11, Supporting Information). In all six ^{1}H NMR spectra, the peaks of washing solvent EtOH were not present, indicating that MOFs were fully activated, and no solvent remained. These results confirm the high purity of all MOFs synthesized at scale. In addition, the good agreement between the calculated and found elemental compositions of all MOF samples (section "Experimental Methods and Materials") indicates that all impurities were removed and no water or EtOH was left in the activated MOFs.

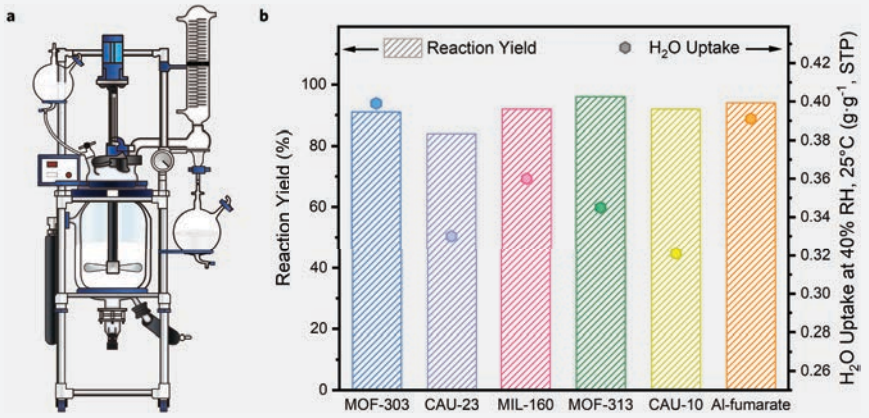

Figure 1. Synthesis of water-harvesting MOFs under reflux conditions in a 200 L reaction vessel. (a) Schematic representation of the experimental setup, as reported in our previous paper[22]. (b) Comparison of the reaction yields and water uptakes at 40% RH and 25°C for scaled-up MOF samples.

Next, the permanent porosity of the aluminum MOF series was investigated using nitrogen sorption analysis (Figure 2b). The Brunauer–Emmett–Teller (BET) surface areas and specific pore volumes of the compounds ranged from 1379 to 654 m^2/g and 0.47 to 0.23 cm^3/g, respectively (Figure S13–S24, Supporting Information). These results are comparable

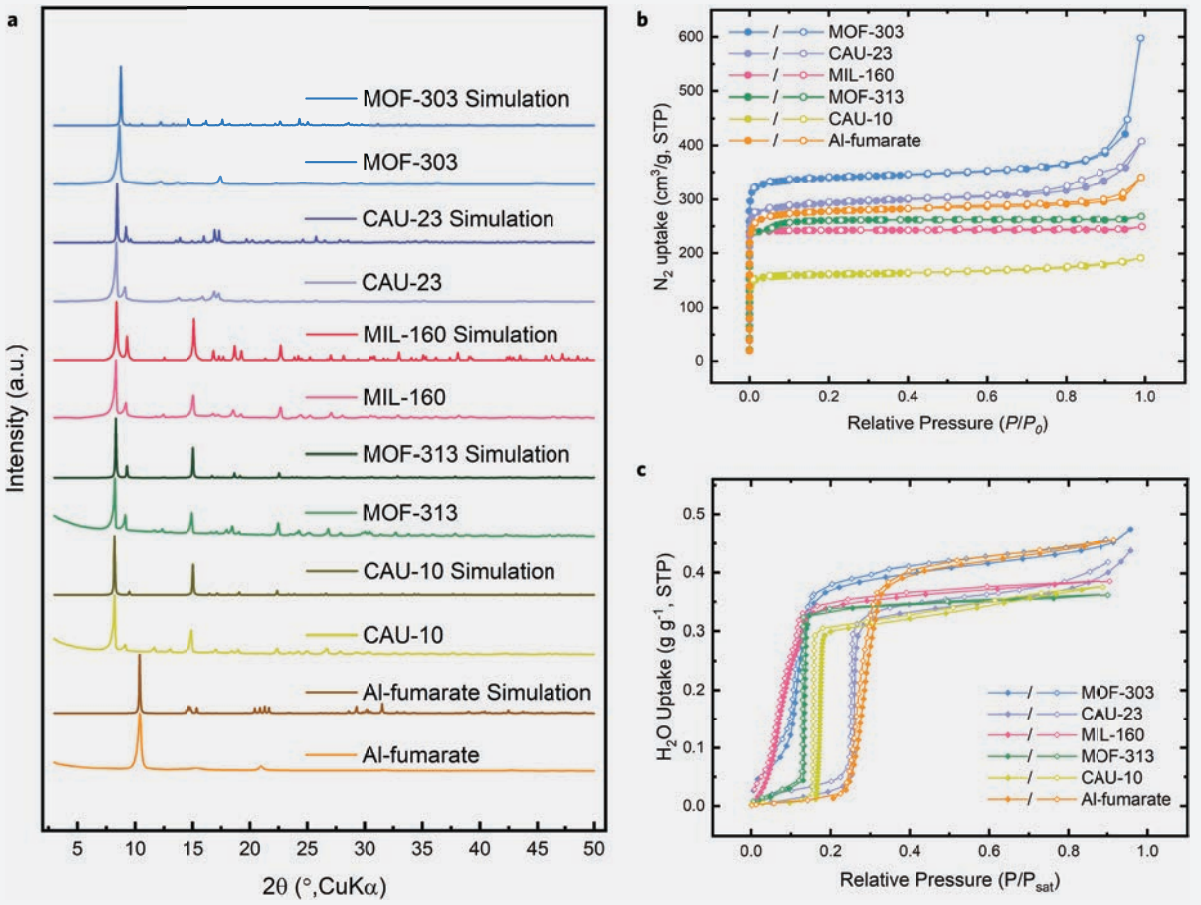

Figure 2. Characterization and sorption measurement of MOFs synthesized at scale. (a) PXRD analysis using Cu Kα radiation. The simulated patterns were calculated using the crystal structures reported in the literature[24,26,31–33]. (b) Nitrogen sorption isotherms (T = 77 K). (c) Water sorption isotherms (T = 25°C). Filled circles depict adsorption; open circles indicate desorption.

to literature data,[6,10,16,26,35] and demonstrate that all scaled-up MOF samples had optimal BET surface areas, pore diameters, and pore volumes (Table S1, Supporting Information). The thermal stability of these MOFs was also evaluated using TGA, and they showed no weight loss up to ~400°C under nitrogen atmospheres (Section S5, Supporting Information).

Finally, we measured the water vapor sorption isotherms of the scaled-up MOF products at 25°C (Figure 2c). All samples showed a consistent S-shaped profile with different steps and water uptake capacities (Table S2, Supporting Information). MOF-303 had an inflection point at 12% RH and the highest gravimetric water capacity of 39 wt% at 40% RH among all six MOFs. This can be attributed to its highest pore volume among the MOFs (Figure S25, Supporting Information). CAU-23 had an inflection point at 26% RH and water capacity of 33 wt% at 40% RH, which was due to the hydrophobic nature of TDC linker (Figure S26, Supporting Information). MIL-160 had the lowest inflection point at 7% RH and gravimetric water capacity of 36 wt% due to its hydrophilic pore environment (Figure S27, Supporting Information). MOF-313 had an inflection point at 13% RH and a gravimetric water capacity of 34 wt%, as for MOF-303 (Figure S28, Supporting Information). CAU-10 had an inflection point at 17% RH and a gravimetric water capacity of 32 wt% because of its smaller pore volume established by bulkier IPA linker (Figure S29, Supporting Information). Al-fumarate had an inflection point at 27% RH and the gravimetric water capacity of 39 wt% (Figure S30, Supporting Information). For most samples, only a small degree of hysteresis was observed between the adsorption and desorption curves, indicating that the optimal conditions (e.g., reaction time, reaction temperature, etc.) minimized the number of defective sites within the crystal lattice. These results show that the water isotherm behavior of

all six aluminum-based MOFs prepared at kilogram scale is comparable to that reported at gram or milligram scale in the literature, and our synthesis method leads to high-quality water harvesting MOF materials at scale.

CONCLUSIONS

In this work, we demonstrated that a series of important water harvesting MOFs (MOF-303, CAU-23, MIL-160, MOF-313, CAU-10, and Al-fumarate) can be synthesized under industrially suitable, green conditions using inexpensive, commercially available linkers. Our facile and robust synthesis method led to production of MOFs at the kilogram scale without compromising framework crystallinity, porosity, or water-harvesting properties. These results demonstrate the feasibility of commercializing MOFs as water-harvesting sorbents and will contribute to the widespread adoption of water-harvesting technologies in the future.

ACKNOWLEDGMENTS

We acknowledge the financial support from Defense Advanced Research Projects Agency (DARPA) under contract HR0011-21-C-0020. Any opinions, findings, and conclusions or recommendations expressed in this material are those of the author(s) and do not necessarily reflect the views of DARPA. ZZ thanks members of the Yaghi Group: Dr. Nikita Hanikel for water isotherm measurements, and Drs. Ha L. Nguyen, Wentao Xu, and Daria Kurandina for helpful discussions. We acknowledge the College of Chemistry Nuclear Magnetic Resonance Facility for resource instruments, which are partially supported by NIH S10OD024998, and staff assistance from Dr. Hasan Celik. We thank Dr. Nick Settineri for his assistance in measuring powder X-ray diffraction patterns. ZZ thanks for the financial support through a Kavli ENSI Graduate Student Fellowship.

NOTE

The authors declare the following competing financial interest(s): Omar M. Yaghi is a co-founder of ATOCO, Inc., aiming at commercializing related technologies.

REFERENCES

1. Bagheri, F. Performance investigation of atmospheric water harvesting systems. *Water Resour. Ind.* **20**, 23–28 (2018).
2. Mekonnen, M.M. & Hoekstra, A.Y. Four billion people facing severe water scarcity. *Sci. Adv.* **2**, e1500323 (2016).
3. Oelkers, E.H., Hering, J.G. & Zhu, C. Water: is there a global crisis? *Elements* **7**, 157–162 (2011).
4. Shannon, M.A. *et al.* Science and technology for water purification in the coming decades. *Nanosci. Technol.* 337–346 (2010).
5. Furukawa, H. *et al.* Water adsorption in porous metal–organic frameworks and related materials. *J. Am. Chem. Soc.* **136**, 4369–4381 (2014).
6. Kim, H. *et al.* Adsorption-based atmospheric water harvesting device for arid climates. *Nat. Commun.* **9**, 1–8 (2018).
7. Xu, W. & Yaghi, O.M. Metal–organic frameworks for water harvesting from air, anywhere, anytime. *ACS Cent. Sci.* **6**, 1348–1354 (2020).
8. Zhou, X., Lu, H., Zhao, F. & Yu, G. Atmospheric water harvesting: a review of material and structural designs. *ACS Mater. Lett.* **2**, 671–684 (2020).
9. Hanikel, N., Prévot, M.S. & Yaghi, O.M. MOF water harvesters. *Nat. Nanotechnol.* **15**, 348–355 (2020).
10. Hanikel, N. *et al.* Rapid cycling and exceptional yield in a metal–organic framework water harvester. *ACS Cent. Sci.* **5**, 1699–1706 (2019).
11. Yang, P., Clark, D.S. & Yaghi, O.M. Envisioning the "Air Economy"—Powered by reticular chemistry and sunlight for clean air, clean energy, and clean water. *Mol. Front. J.* **5**, 30–37 (2021).
12. Kim, H. *et al.* Water harvesting from air with metal–organic frameworks powered by natural sunlight. *Science* **356**, 430–434 (2017).
13. Fathieh, F. *et al.* Practical water production from desert air. *Sci. Adv.* **4**, eaat3198 (2018).
14. Yilmaz, G. *et al.* Autonomous atmospheric water seeping MOF matrix. *Sci. Adv.* **6**, eabc8605 (2020).
15. Burtch, N.C., Jasuja, H. & Walton, K.S. Water stability and adsorption in metal–organic frameworks. *Chem. Rev.* **114**, 10575–10612 (2014).
16. Lenzen, D. *et al.* Scalable green synthesis and full-scale test of the metals and fullon, K. S. Wa-10-H for use in adsorption-driven chillers. *Adv. Mater.* **30**, 1705869 (2018).
17. Kim, S.-N., Lee, Y.-R., Hong, S.-H., Jang, M.-S. & Ahn, W.-S. Pilot-scale synthesis of a zirconium-benzenedicarboxylate UiO-66 for CO2 adsorption and catalysis. *Catal. Today* **245**, 54–60 (2015).
18. Rubio-Martinez, M. *et al.* Scalability of continuous flow production of metalrboxylate UiO-66 for *ChemSusChem* **9**, 938–941 (2016).
19. DeSantis, D. *et al.* Techno-economic analysis of metal–organic frameworks for hydrogen and natural gas storage. *Energy Fuels* **31**, 2024–2032 (2017).
20. Gaab, M., Trukhan, N., Maurer, S., Gummaraju, R. & Müller, U. The progression of Al-based metal-organic frameworks—From academic research to industrial

production and applications. *Microporous Mesoporous Mater.* **157**, 131–136 (2012).
21. Khabzina, Y. *et al.* Synthesis and shaping scale-up study of functionalized UiO-66 MOF for ammonia air purification filters. *Ind. Eng. Chem. Res.* **57**, 8200–8208 (2018).
22. Zheng, Z., Hanikel, N., Lyu, H. & Yaghi, O.M. Broadly tunable atmospheric water harvesting in multivariate metal–organic frameworks. *J. Am. Chem. Soc.* **144**, 22669–22675 (2022).
23. Zheng, Z. *et al.* High-yield, green and scalable methods for producing MOF-303 for water harvesting from desert air. *Nat. Protoc.* **18**, 136–156 (2023).
24. Lenzen, D. *et al.* A metal-organic framework for efficient water-based ultra-low-temperature-driven cooling. *Nat. Commun.* **10**, 1–9 (2019).
25. Cadiau, A. *et al.* Design of hydrophilic metal organic framework water adsorbents for heat reallocation. *Adv. Mater.* **27**, 4775–4780 (2015).
26. Cho, K.H. *et al.* Rational design of a robust aluminum metal-organic framework for multi-purpose water-sorption-driven heat allocations. *Nat. Commun.* **11**, 1–8 (2020).
27. Yaghi, O.M., Hanikel, N. & Hao, L. Multivariate and other metal-organic frameworks, and uses thereof. U.S. Patent No. 62/771,537, University of California (2020).
28. Leung, E. *et al.* Process for preparing porous metal-organic frameworks based on aluminum fumarate. U.S. Patent No. 8,524,932, BASF SE patent (2013).
29. Kiener, C., Müller, U. & Schubert, M. Method of using a metal organic frameworks based on aluminum fumarate. U. S. Patent No. 8,518,264. (2013).
30. Reinsch, H. *et al.* Structures, sorption characteristics, and nonlinear optical properties of a new series of highly stable aluminum MOFs. *Chem. Mater.* **25**, 17–26 (2013).
31. Alvarez, E. *et al.* The structure of the aluminum fumarate metal–organic framework A520. *Angew. Chem.* **127**, 3735–3739 (2015).
32. Fröhlich, D. *et al.* Water adsorption behaviour of CAU-10-H: a thorough investigation of its structure–property relationships. *J. Mater. Chem. A.* **4**, 11859–11869 (2016).
33. Hanikel, N. *et al.* Evolution of water structures in metal-organic frameworks for improved atmospheric water harvesting. *Science* **374**, 454–459 (2021).
34. Zheng, Z. *et al.* High-yield, green and scalable methods for producing MOF-303 for water harvesting from desert air. *Nat. Protoc.*, 1–21 (2022).
35. Tannert, N., Jansen, C., Nießing, S. & Janiak, C. Robust synthesis routes and porosity of the Al-based metal–organic frameworks Al-fumarate, CAU-10-H and MIL-160. *Dalton Trans.* **48**, 2967–2976 (2019).
36. Lenzen, D. *et al.* A metal–organic framework for efficient water-based ultra-low-temperature-driven cooling. *Nat. Commun.* **10**, 3025 (2019).
37. Lee, J.S. *et al.* Porous metal–organic framework CUK-1 for adsorption heat allocation toward green applications of natural refrigerant water. *ACS Appl. Mater. Interfaces* **11**, 25778–25789 (2019).
38. Zhao, T. *et al.* High-yield, fluoride-free and large-scale synthesis of MIL-101 (Cr). *Dalton Trans.* **44**, 16791–16801 (2015).
39. Sohail, M. *et al.* Synthesis of highly crystalline NH2-MIL-125 (Ti) with S-shaped water isotherms for adsorption heat transformation. *Cryst. Growth Des.* **17**, 1208–1213 (2017).
40. Permyakova, A. *et al.* Synthesis optimization, shaping, and heat reallocation evaluation of the hydrophilic metal–organic framework MIL-160 (Al). *ChemSusChem* **10**, 1419–1426 (2017).
41. Wang, S. *et al.* A robust large-pore zirconium carboxylate metal–organic framework for energy-efficient water-sorption-driven refrigeration. *Nat. Energy* **3**, 985–993 (2018).
42. Rieth, A.J., Yang, S., Wang, E.N. & Dincă, M. Record atmospheric fresh water capture and heat transfer with a material operating at the water uptake reversibility limit. *ACS Cent. Sci.* **3**, 668–672 (2017).
43. Czaja, A., Leung, E., Trukhan, N. & Müller, U. Industrial MOF synthesis. *Metal-Organic Frameworks: Applications from Catalysis to Gas Storage*, 337–352 (2011).
44. Reinsch, H. *et al. Chem. Mater* **25**, 17–26 (2013).

SUPPORTING INFORMATION

SECTION S1: POWDER X-RAY DIFFRACTION ANALYSIS

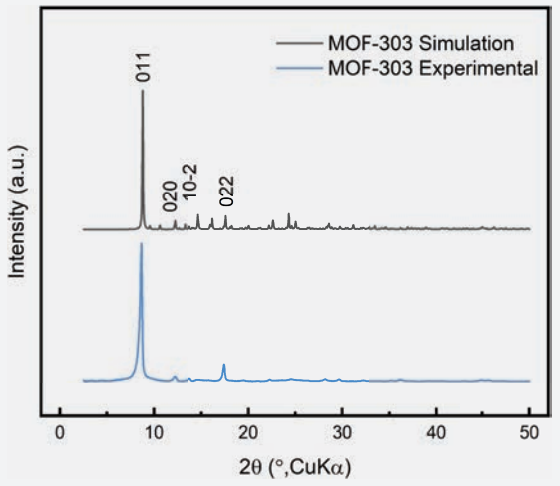

Figure S1. Powder X-ray diffraction analysis of MOF-303.

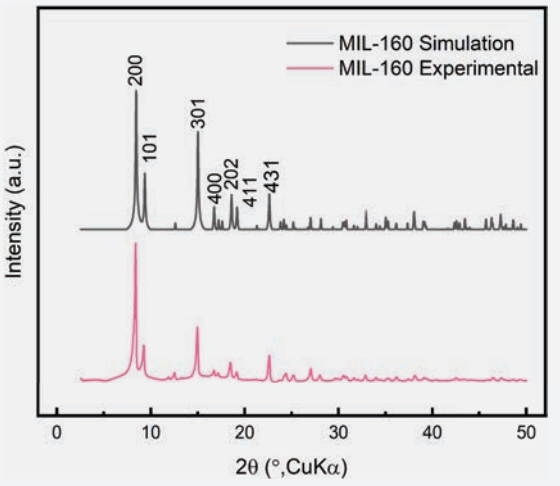

Figure S3. Powder X-ray diffraction analysis of MIL-160.

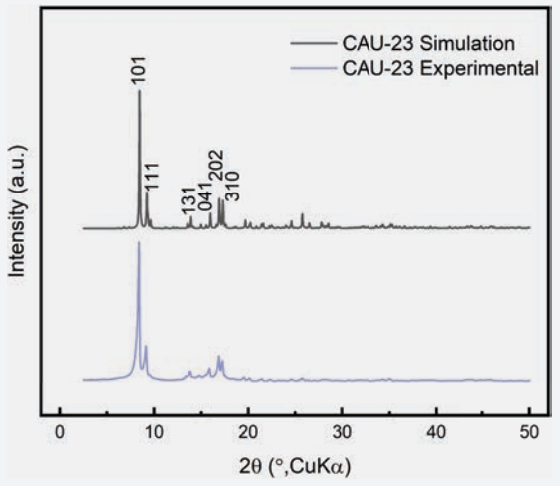

Figure S2. Powder X-ray diffraction analysis of CAU-23.

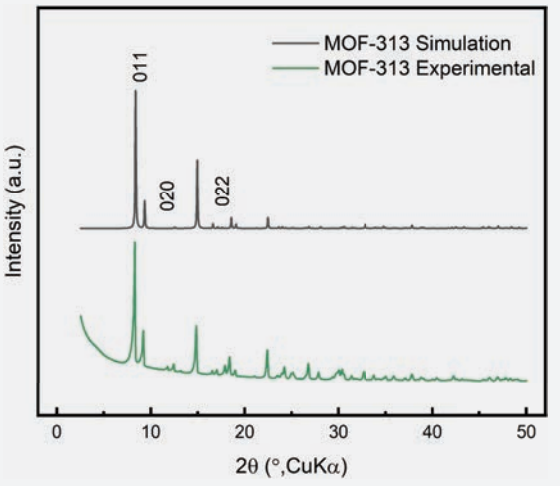

Figure S4. Powder X-ray diffraction analysis of MOF-313.

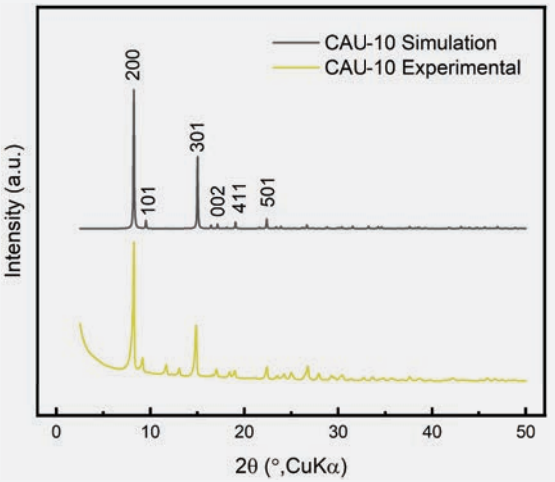

Figure S5. Powder X-ray diffraction analysis of CAU-10.

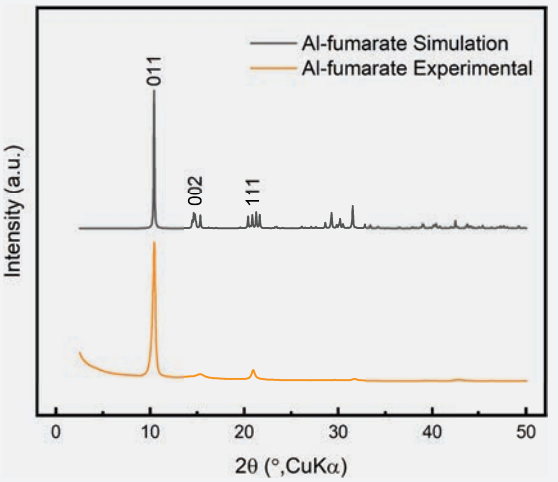

Figure S6. Powder X-ray diffraction analysis of Al-fumarate.

SECTION S2: NUCLEAR MAGNETIC RESONANCE SPECTROSCOPY

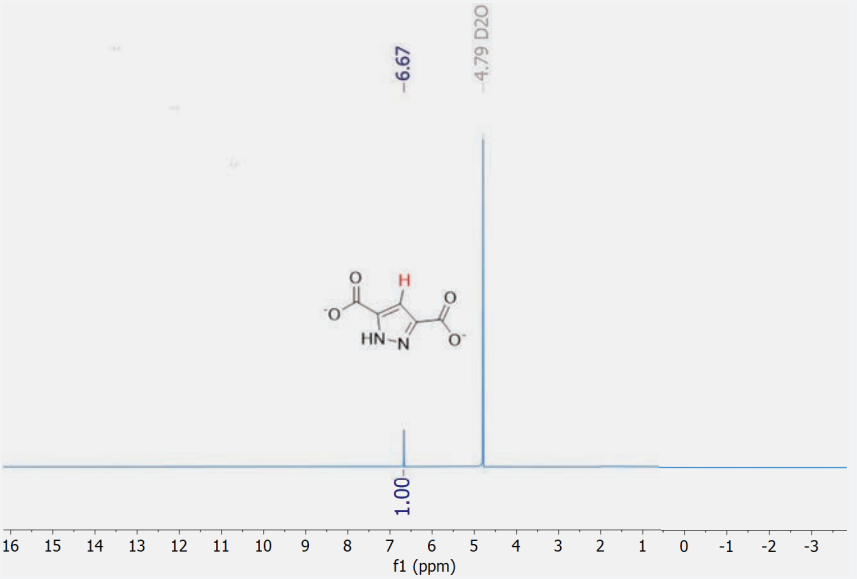

Figure S7. ^{1}H-NMR spectrum of MOF-303 after being thoroughly washed with EtOH and digested in 10% NaOD in D_2O.

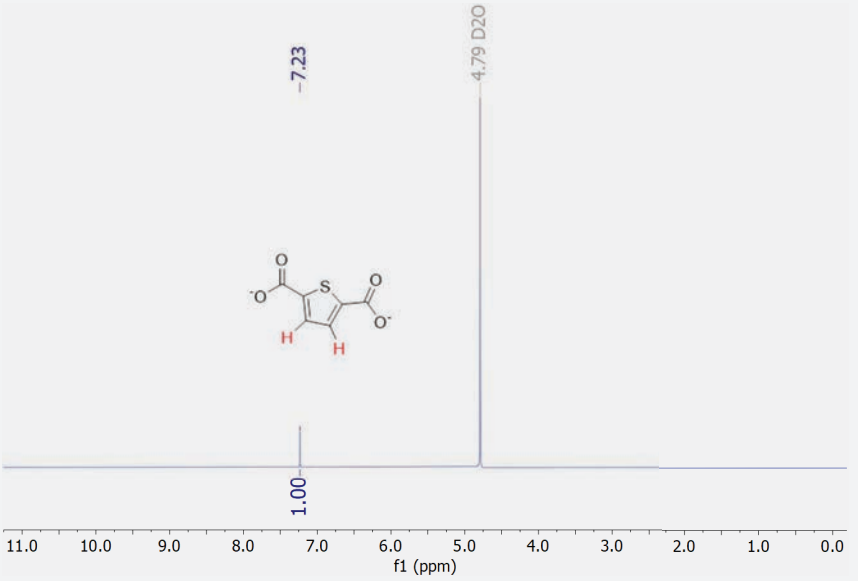

Figure S8. ^{1}H-NMR spectrum of CAU-23 after being thoroughly washed with EtOH and digested in 10% NaOD in D_2O.

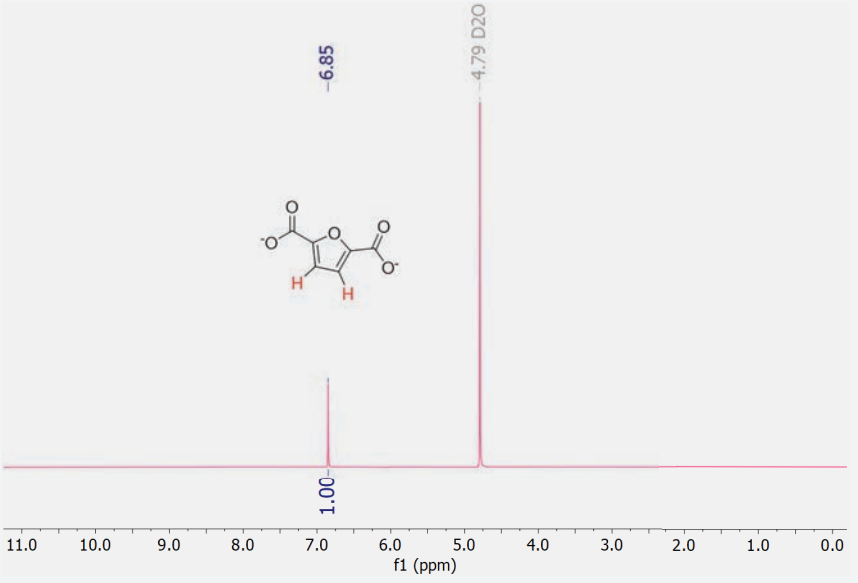

Figure S9. ^{1}H-NMR spectrum of MIL-160 after being thoroughly washed with EtOH and digested in 10% NaOD in D_2O.

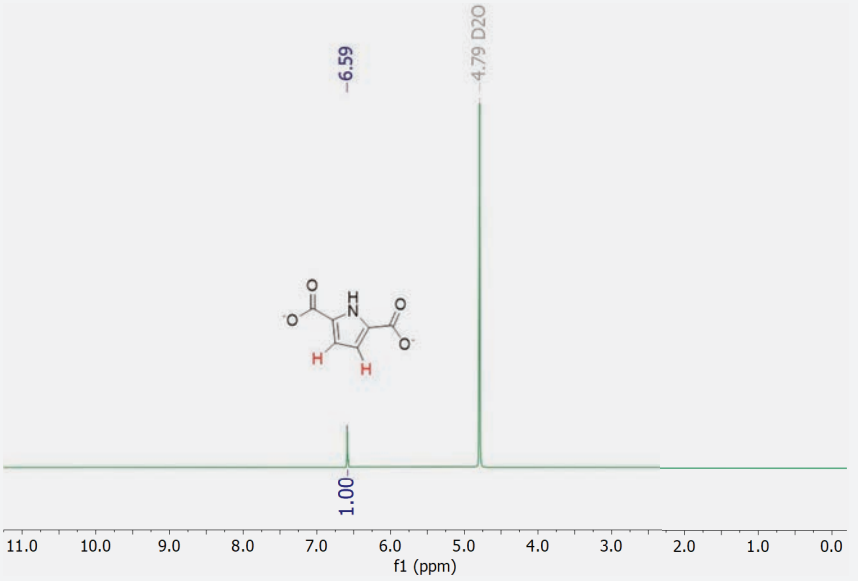

Figure S10. ^{1}H-NMR spectrum of MOF-313 after being thoroughly washed with EtOH and digested in 10% NaOD in D_2O.

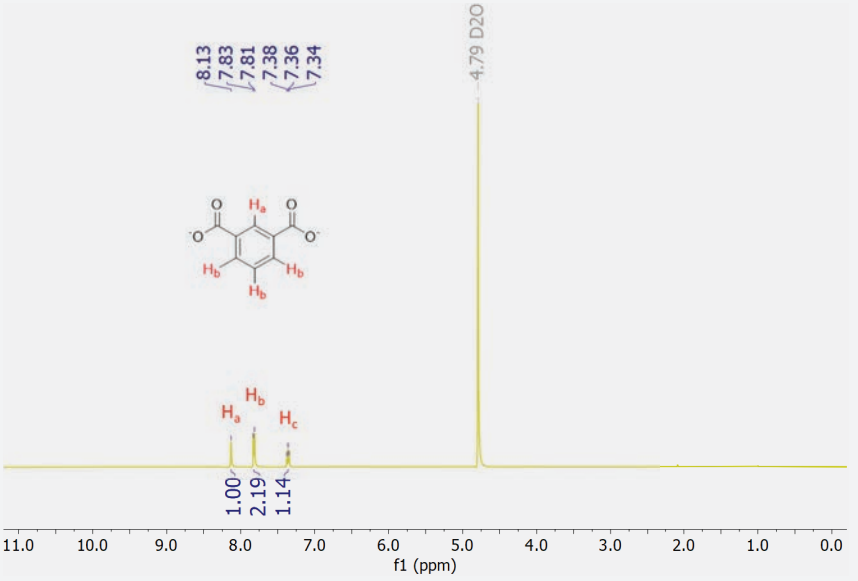

Figure S11. ^{1}H-NMR spectrum of CAU-10 after being thoroughly washed with EtOH and digested in 10% NaOD in D_2O.

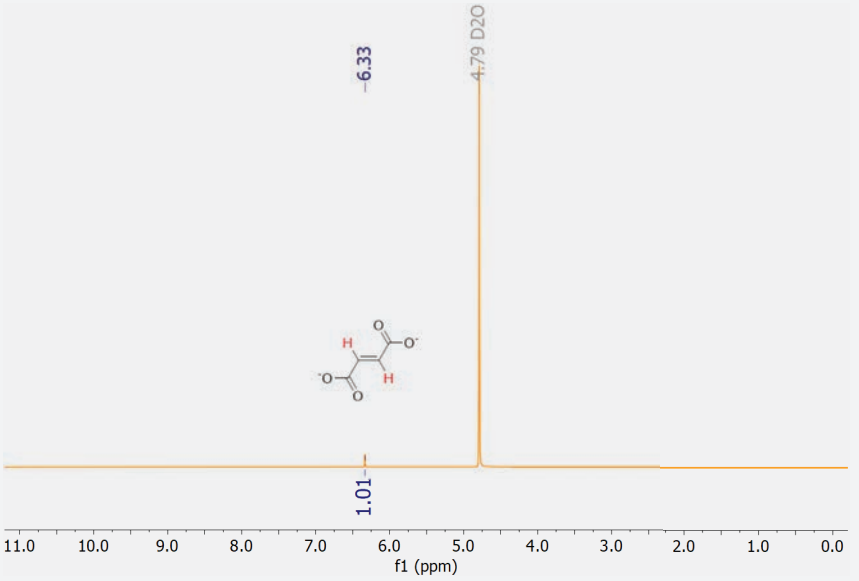

Figure S12. ^{1}H-NMR spectrum of Al-fumarate after being thoroughly washed with EtOH and digested in 10% NaOD in D_2O.

SECTION S3: NITROGEN SORPTION ANALYSIS

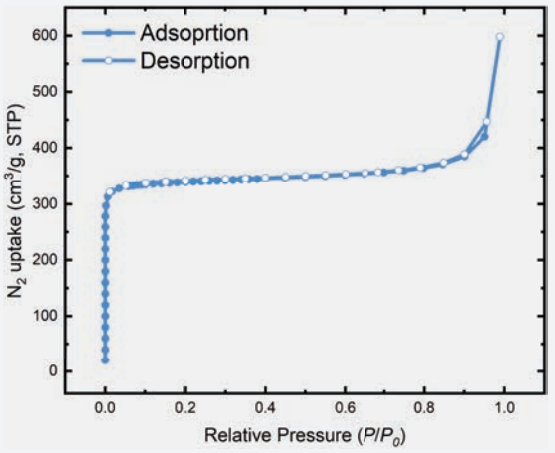

Figure S13. Nitrogen sorption analysis of MOF-303 at 77K (BET surface area 1,379 m^2/g; P: partial pressure of argon, P_0 = 1 atm, STP: standard temperature and pressure).

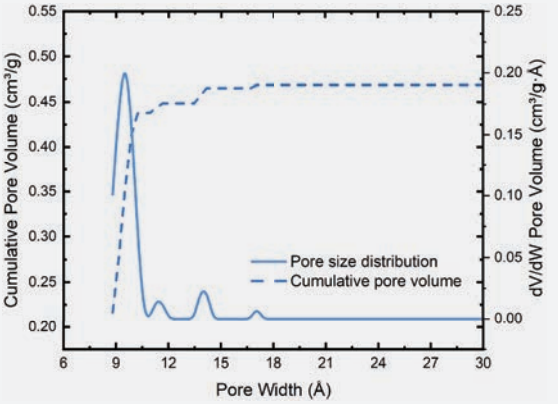

Figure S14. Differential and cumulative pore volume of MOF-303 estimated from its nitrogen sorption isotherm at 77 K.

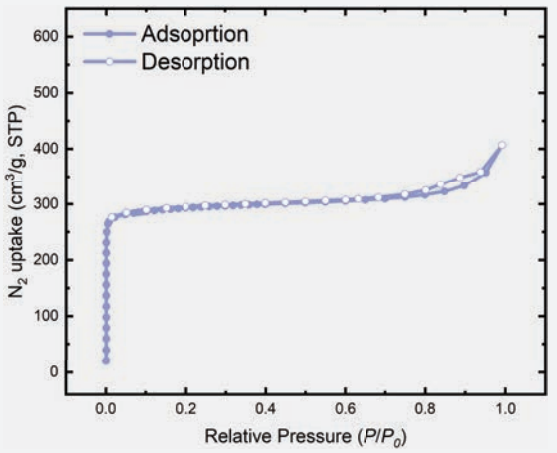

Figure S15. Nitrogen sorption analysis of CAU-23 at 77K (BET surface area 1,176 m^2/g; P: partial pressure of argon, P_0 = 1 atm, STP: standard temperature and pressure).

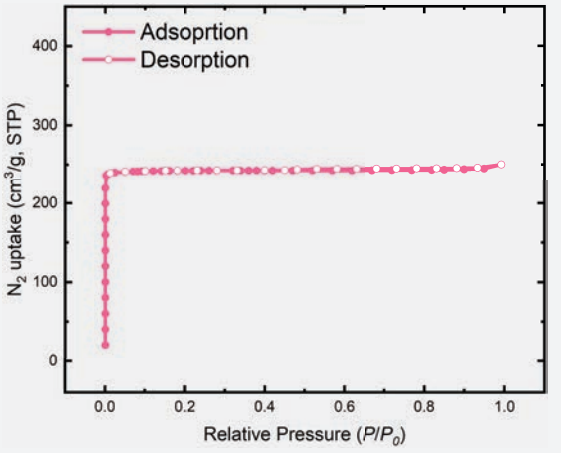

Figure S17. Nitrogen sorption analysis of MIL-160 at 77K (BET surface area 1,030 m^2/g; P: partial pressure of argon, P_0 = 1 atm, STP: standard temperature and pressure).

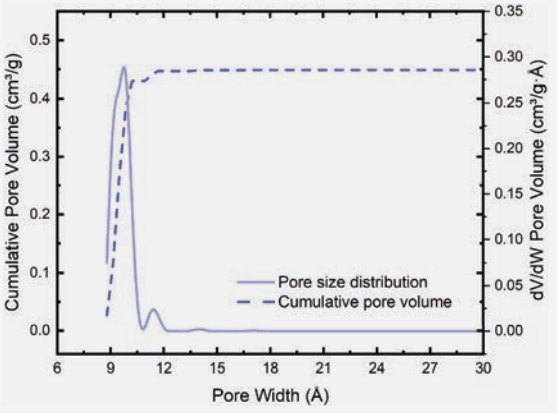

Figure S16. Differential and cumulative pore volume of CAU-23 estimated from its nitrogen sorption isotherm at 77 K.

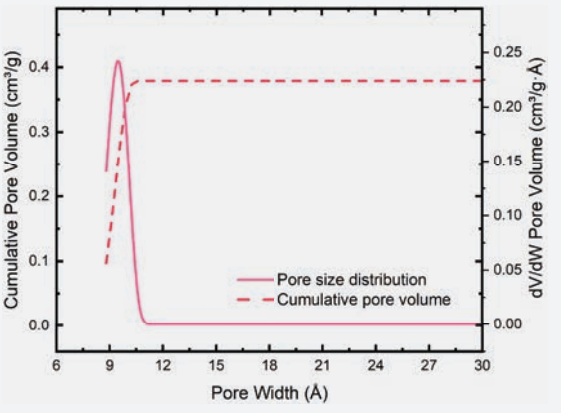

Figure S18. Differential and cumulative pore volume of MIL-160 estimated from its nitrogen sorption isotherm at 77 K.

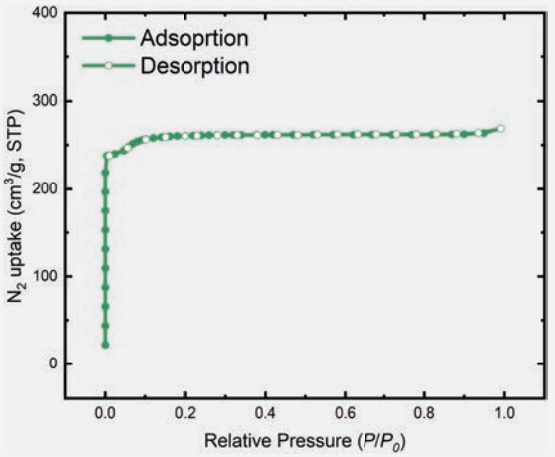

Figure S19. Nitrogen sorption analysis of MOF-313 at 77K (BET surface area 1,033 m^2/g; P: partial pressure of argon, P_0 = 1 atm, STP: standard temperature and pressure).

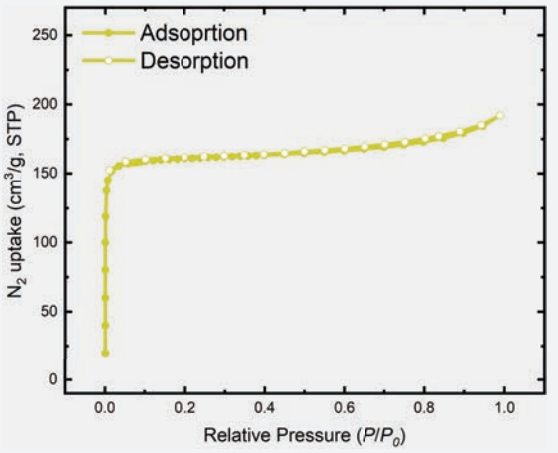

Figure S21. Nitrogen sorption analysis of CAU-10 at 77K (BET surface area 654 m^2/g; P: partial pressure of argon, P_0 = 1 atm, STP: standard temperature and pressure).

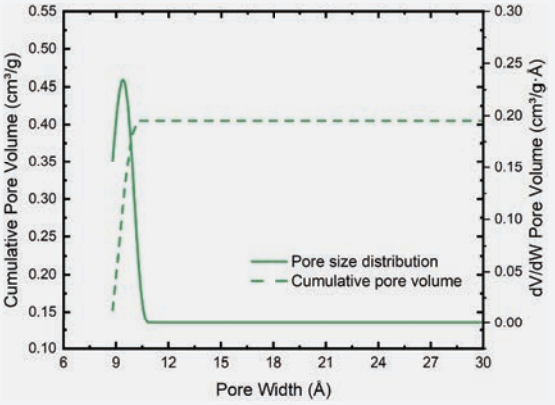

Figure S20. Differential and cumulative pore volume of MOF-313 estimated from its nitrogen sorption isotherm at 77 K.

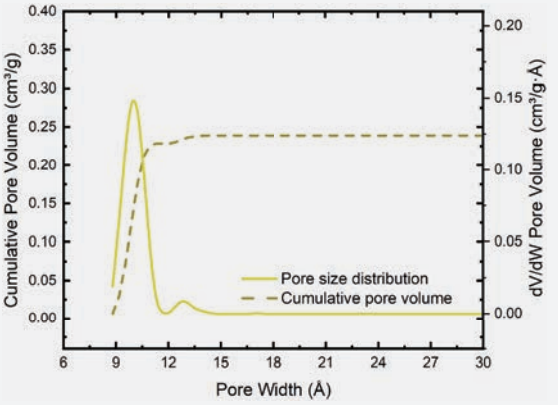

Figure S22. Differential and cumulative pore volume of CAU-10 estimated from its nitrogen sorption isotherm at 77 K.

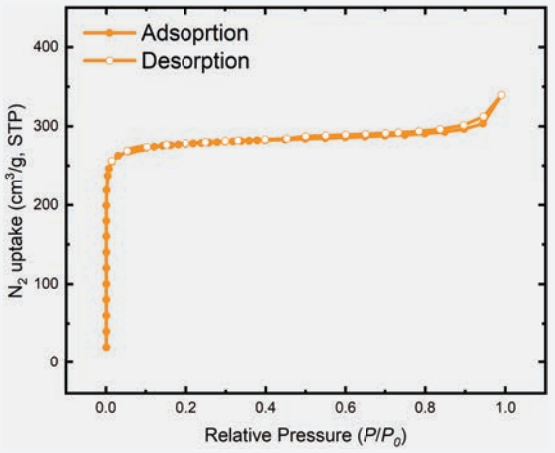

Figure S23. Nitrogen sorption analysis of Al-fumarate at 77K (BET surface area 1,108 m^2/g; P: partial pressure of argon, P_0 = 1 atm, STP: standard temperature and pressure).

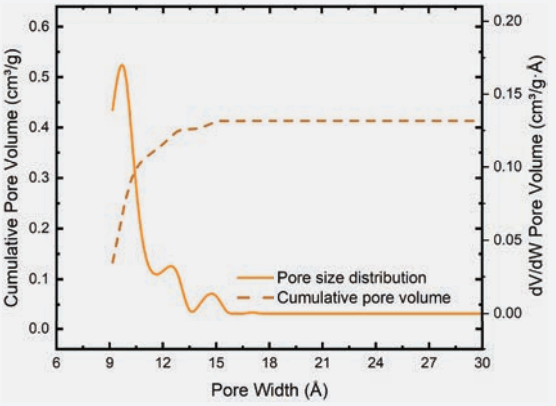

Figure S24. Differential and cumulative pore volume of Al-fumarate estimated from its nitrogen sorption isotherm at 77 K.

Table S1. Summary of the results from the nitrogen sorption analysis on the water-harvesting MOF series (Figs. S13 to S24). Standard deviations (where available) are expressed in brackets in terms of the least significant digit.

MOF	BET surface area (m^2/g)	Pore volume calculated by DFT (cm^3/g)	Pore size calculated by DFT (Å)
MOF-303	1379(1)	0.471	9.54
CAU-23	1176(2)	0.450	9.68
MIL-160	1030(2)	0.381	9.54
MOF-313	1033(4)	0.405	9.40
CAU-10	654(2)	0.239	10.01
Al-fumarate	1108(4)	0.410	9.84

SECTION S4: WATER SORPTION ANALYSIS

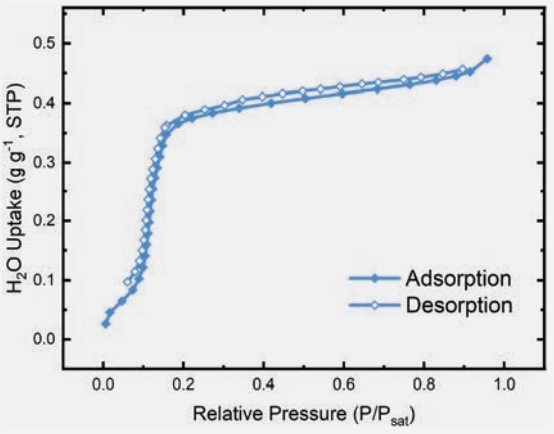

Figure S25. Water vapor sorption isotherms of MOF-303 against relative humidity at 25°C (P: partial water vapor pressure, P_{sat}: saturation water vapor pressure at 25°C, STP: standard temperature and pressure).

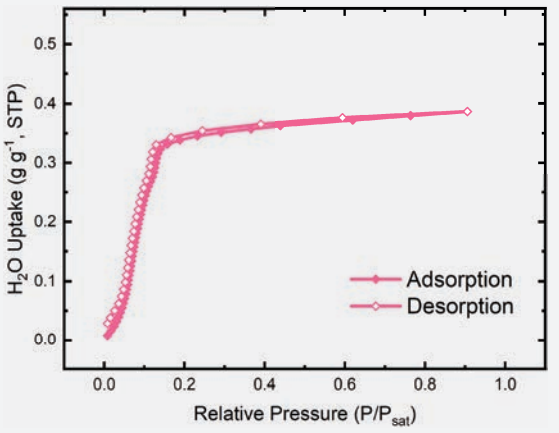

Figure S27. Water vapor sorption isotherms of MIL-160 against relative humidity at 25°C (P: partial water vapor pressure, P_{sat}: saturation water vapor pressure at 25°C, STP: standard temperature and pressure).

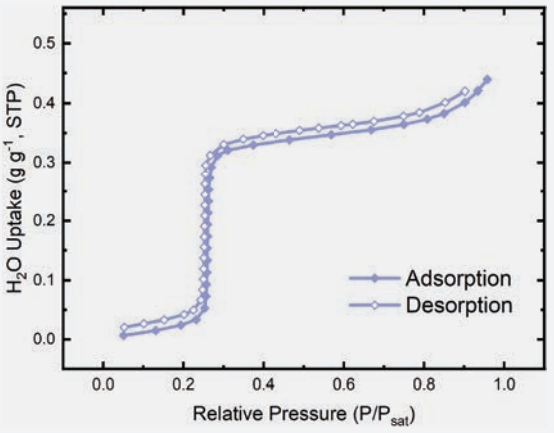

Figure S26. Water vapor sorption isotherms of CAU-23 against relative humidity at 25°C (P: partial water vapor pressure, P_{sat}: saturation water vapor pressure at 25°C, STP: standard temperature and pressure).

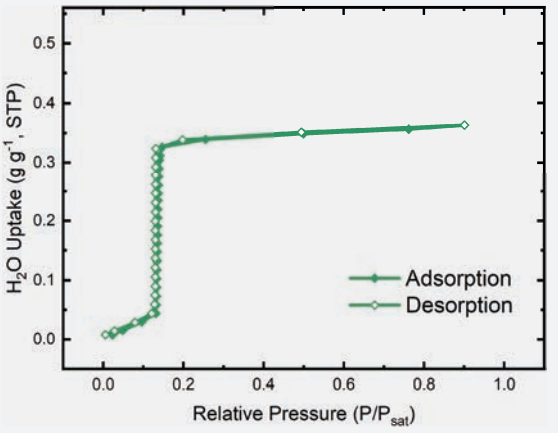

Figure S28. Water vapor sorption isotherms of MOF-313 against relative humidity at 25°C (P: partial water vapor pressure, P_{sat}: saturation water vapor pressure at 25°C, STP: standard temperature and pressure).

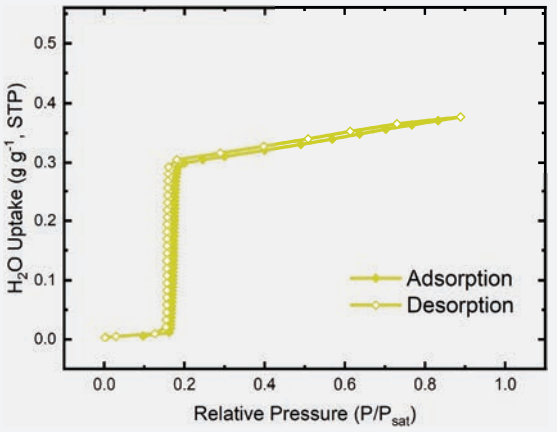

Figure S29. Water vapor sorption isotherms of CAU-10 against relative humidity at 25°C (P: partial water vapor pressure, P_{sat}: saturation water vapor pressure at 25°C, STP: standard temperature and pressure).

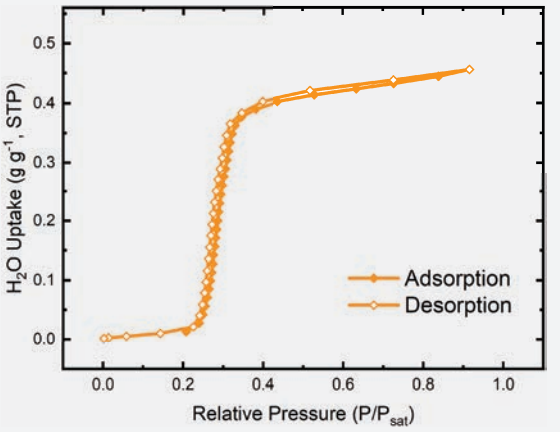

Figure S30. Water vapor sorption isotherms of Al-fumarate against relative humidity at 25°C (P: partial water vapor pressure, P_{sat}: saturation water vapor pressure at 25°C, STP: standard temperature and pressure).

Table S2. Summary of the results from the water sorption isotherms on the water-harvesting MOF series (Figs. S25 to S30).

MOF	Step (% RH)	Capacity (g/g)
MOF-303	12	0.39
CAU-23	26	0.33
MIL-160	7	0.36
MOF-313	13	0.34
CAU-10	17	0.32
Al-fumarate	27	0.39

SECTION S5: THERMOGRAVIMETRIC ANALYSIS

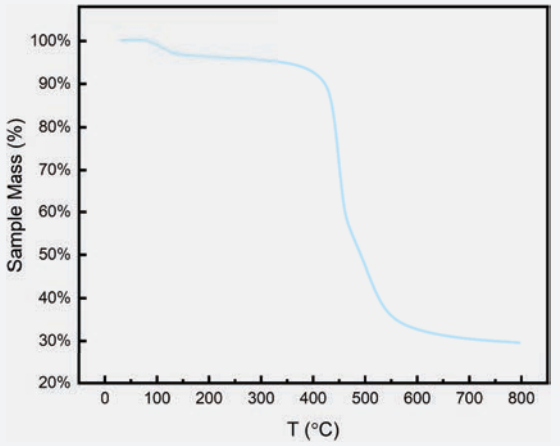

Figure S31. TGA profile of MOF-303 measured under N_2 flow.

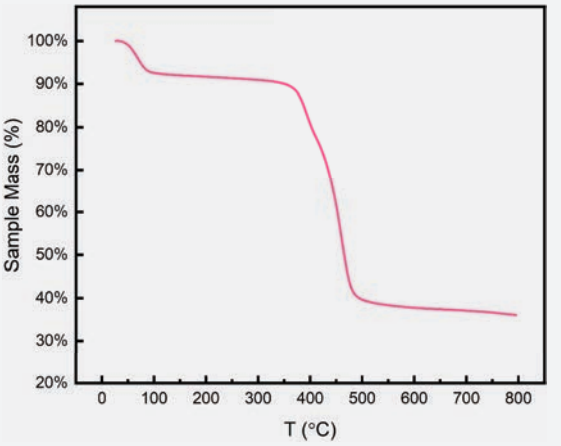

Figure S33. TGA profile of MIL-160 measured under N_2 flow.

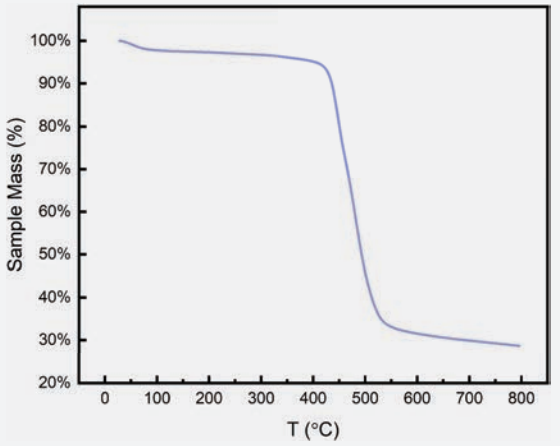

Figure S32. TGA profile of CAU-23 measured under N_2 flow.

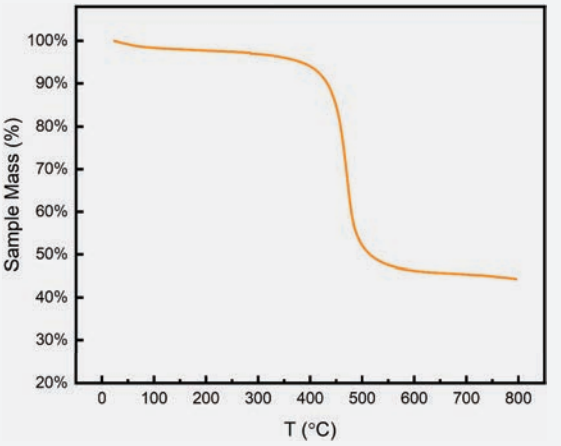

Figure S34. TGA profile of Al-fumarate measured under N_2 flow.